

Optimized synthesis for improved TiO₂ NT array surface

(Otimização do processo de síntese de NT de TiO₂ visando a obtenção de uma melhor qualidade de superfície)

P. A. Marques¹, K. F. Albertin^{2*}, G. Z. Monteiro¹, I. Pereyra¹

¹Universidade de São Paulo, LME/PSI/EPUSP, 05508-900, S. Paulo, SP, Brazil

²Universidade Federal do ABC, CECS, 09210-170, Santo André, SP, Brazil

Abstract

Different thicknesses of photoresist layers were deposited on the Ti foil in order to decrease the initial current during the anodization process, avoiding or diminishing in this way the formation of the initial compact TiO₂ layer. The studies of the initial synthesis stages were performed in both cases, for the conventional synthesis and for that with photoresist layer on top of the Ti foil. TiO₂ nanotube pH electrodes were fabricated to study the effect of this change in the anodization process. The nanostructure morphology was analyzed through scanning electron microscopy technique. Total removal of the undesirable layer and a complete release of the nanotube mouth were obtained. The pH electrodes were characterized utilizing a buffer solution and improved pH sensitivity and absence of hysteresis effects were observed for the devices fabricated with TiO₂ nanotubes obtained with the optimized process.

Keywords: TiO₂ nanotube arrays, morphology, initial nucleation layer, photoresist layer.

Resumo

Diferentes espessuras de camadas de fotorresiste foram depositadas sobre a lâmina de Ti, de forma a diminuir a corrente inicial durante o processo de síntese e, assim, evitar ou reduzir a formação da camada inicial compacta de TiO₂ sobre os nanotubos. Foi realizado um estudo dos estágios iniciais de crescimento dos nanotubos (NTs) para a síntese convencional e com a presença das camadas de fotorresiste. Os NTs de TiO₂ foram caracterizados pela técnica de microscopia eletrônica de varredura. Eletrodos de pH foram fabricados com os NTs obtidos e foram caracterizados. Notou-se a total ausência da camada porosa de TiO₂ com o uso da camada de fotorresiste e os eletrodos de pH apresentaram melhora em sua sensibilidade e a ausência do efeito de histerese quando comparados aos fabricados com os nanotubos crescidos sem a camada de fotorresiste.

Palavras-chave: matrizes de nanotubos de TiO₂, morfologia, camada inicial, camada de fotorresiste.


INTRODUCTION

Titanium dioxide (TiO₂) is an n-type semiconductor that has attracted great interest due to its wide band gap, photosensitivity, non-toxicity, low-cost and high thermal and chemical stability [1, 2]. Furthermore, it is a promising material for nanotemplating, photocatalytic, photovoltaic, photoelectrolysis and sensing applications [3, 4]. These outstanding properties stimulated the production of different TiO₂ morphologies. Several structures have been obtained such as nanoparticles and nanotubes. Among these, nanotubular structures present a larger surface area, higher light-harvesting and less electron recombination than TiO₂ nanoparticles [5]. From the fabrication point of view, titanium dioxide nanotubes are obtained through various processes as sol-gel technique, geminated growth, and hydrothermal process. However, Ti foil electrochemical anodization in fluorinated solutions has demonstrated to be one of the best techniques to obtain highly ordered and high

aspect ratio structures with a well-defined and controllable diameter, wall thickness and tube length.

The performance of devices based on TiO₂ is affected by the shape and size of the TiO₂ nanotubes. For example, the TiO₂ nanotube electrodes have better sensitivity towards pH than thin film electrodes because of their high surface area and abundant hydroxyl groups on its surface [6]. However, during the anodization process, an initial nanoporous layer often remains as residue, also bundles of clumped remnants could be produced at the nanotube tops [7], as shown in Fig. 1, prejudicing device performance. The characteristics of these remnants depend on the anodization voltage and time since for each applied voltage (keeping the other parameters constant such as pH, agitation, temperature, and electrolyte composition) exists a limit anodization time to avoid disordered top layers [8]. To understand the cause of this limit time for each different applied voltage, an interpretation of the growth mechanism is needed. The anodic oxide growth process has two main reactions: field-assisted oxidation and chemical dissolution. Initially, the applied electric field transports hydroxyl ions (OH⁻) from the electrolyte to the titanium metallic interface and these

*katia.torres@ufabc.edu.br

 <https://orcid.org/0000-0002-5774-695X>

ions react with the metal surface to form a compact oxide layer. At the same time, the chemical dissolution of the oxide occurs when there are fluoride ions in the electrolyte. This late reaction originates the initial porous layer formation and, for increasing process time, the NTs' self-organized arrangement [9]. The chemical dissolution occurs mainly on the array surface and therefore the dissolution rate remains constant along the process, depending only on the F^- ions concentration. On the other hand, the oxide growth occurs at the TiO_2/Ti interface and therefore its rate decreases as the oxide (TiO_2) thickness increases, being controlled by the diffusion of the OH^- ions through the oxide layer. In this way at the initial stage, the titania formation is faster than its chemical dissolution, but when the oxide thickness increases the diffused OH^- ions at the oxide/metal interface diminish and so the growth rate. As a consequence, for a given oxide thickness and process time, the dissolution rate dominates the growth rate and thus the TiO_2 nanotubes stop growing. As the oxide growth is assisted by an electric field that depends on the applied voltage, this limit time is a function of the applied voltage.

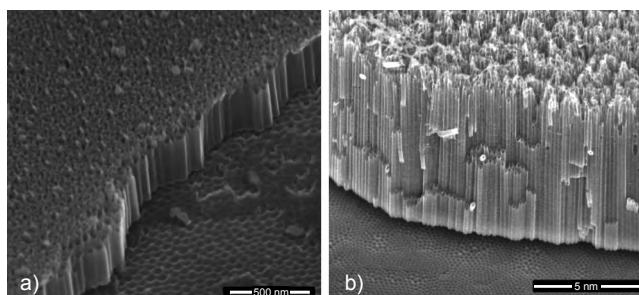


Figure 1: SEM images of TiO_2 NT arrays covered with: a) initial nucleation layer; and b) nanograss layer.

[Figura 1: Imagens de MEV dos nanotubos de TiO_2 com: a) camada inicial de TiO_2 ; e b) camada de nanograma.]

Anodizing voltage is a key factor in the growth kinetics of TiO_2 nanotubes (NTs) because it determines the electric field intensity [10]. Low potential supplies lower driving force for ionic species (H^+ , OH^- and F^-) to move across the barrier layer at the bottom of the nanotubes array, which hampers the ionic mobility of the Ti/TiO_2 interface into the Ti metal [11]. On the other hand, the anodization time affects the length of titania nanotubes, which increases with the anodizing time, provided the anodization process did not extrapolate the limit time previously outlined [12]. In previous studies, it was observed that the titania nanotubes growth is not linear [7, 12, 13], even more, the average growth rate decreased for increasing anodization time due to the imbalance between oxide growth and dissolution for long-time experiments [13-15]. The formation of NT bundles was observed for high anodization voltage, above 60 V, or for long process time, for low voltage values, where dissolution rate dominates the growth rate. For samples grown under low applied potential and time process, a porous layer on the NT top is observed [7]. This is a critical issue for many applications, because

the nano-remnants affect the infiltration of materials, charge transport and recombination in TiO_2 nanotube solar cells and sensors, etc. [16, 17]. In order to avoid the presence of TiO_2 porous layer in the top of NTs, consequently to have the compact TiO_2 layer initial formation, the idea is to utilize a photoresist thin film layer during the anodization process. To understand better the application of the photoresist layer, first is necessary to understand the different growth stages during the anodization process, each of these stages is characterized by a current density vs. anodization time behavior (Fig. 2), where porous oxide (PO) stands for a growth process in the presence of fluorine ions and compact oxide (CO) stands for just plain oxidation without dissolution agent. In this way, the first anodization step (I), where the Ti dioxide compact layer growth occurs, must be eliminated. For this purpose, it is necessary to diminish significantly the initial current density which can be attained with an appropriated photoresist layer. This insulating layer substitutes the compact Ti dioxide layer, formed in the first step (PO), limiting the current and thus making the anodization process to start from stage II with the pits and nanotubes formation [7]. This optimized process can be utilized for low time processes avoiding the presence of the Ti porous membrane and also for long time processes, because the photoresist film layer protects the nanotube mouth from the dissolution process that occurs for long times, avoiding the NT bundles. When NT formation finishes, the photoresist layer is removed.

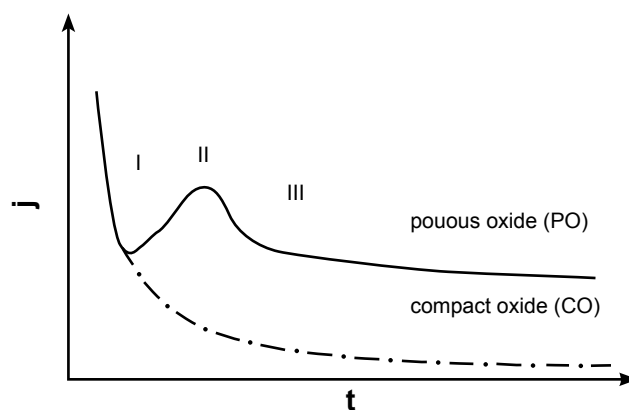


Figure 2: Schematic of characteristic current density vs. anodization time curves (adapted from [7]).

[Figura 2: Esquema de curvas de densidade de corrente em função do tempo de anodização (adaptada de [7]).]

In this way, first a study of the different nanotubes' growth stages was performed in order to understand the mechanism of the TiO_2 initial porous membrane formation and to confirm the idea that this layer remains after TiO_2 NT formation. In sequence, a study of TiO_2 NT synthesis, with a voltage of 60 V, for different times with a photoresist layer was done, aiming to obtain an optimized process, in order to avoid the growth of this initial layer for low anodization times and NT bundles for high anodization times. This is a critical issue for many applications, because both the porous layer and the bundles affect the infiltration

of materials, charge transport and recombination in TiO₂ nanotube solar cells and sensors, etc. [16, 17]. TiO₂ NT arrays were characterized by scanning electron microscopy (SEM) technique. TiO₂ nanotubes arrays obtained with and without photoresist layer were utilized and characterized as pH sensor electrode.

EXPERIMENTAL

Sample preparation: titanium foils (99% purity, Alfa Aesar) were polished using nitric, acetic and hydrofluoric acid solutions in a volume proportion of 3:1:1 for 3 min [18]. In sequence, the foils were immersed in an electrochemical solution consisting basically of a mixture of ethylene glycol+2.56% (volume) of deionized water and 0.146 M of NH₄F solution. The anodization was carried out at controlled temperature (25 °C) and applying a constant voltage of 30 V to obtain TiO₂ NTs, for the study of stages of TiO₂ NT growth, and 60 V for studies to avoid the NT top and disordered layer and its stages of TiO₂ growth. A lower value of voltage was utilized for the study of the different TiO₂ NT growth stages for nanotubes obtained without photoresist in order to permit a more precise observation of the initial NT growth steps that occurred in the few initial seconds. For higher voltages, this step of the growth process occurs very rapidly and thus is difficult to visualize it.

Nanotubes growth process: a positive photoresist (PR) layer (AZ1518) was deposited by spin coating on the Ti surface. The Ti foils were rinsed in isopropyl alcohol and in Table I the parameters utilized to obtain the different insulating layers studied are shown. For a sacrificial layer of 1 μm, the photoresist was diluted in a proportion of 1:4 in a photoresist thinner (1-methoxy-2-propyl acetate 100-65-6). The photoresist softbake was carried out at 100 °C for 30 min. In sequence, the samples were anodized at 60 V for 5, 15 and 30 min and washed with conventional cleaning. To study the different TiO₂ growth stages with 1 μm photoresist layer anodization times of 1, 4, 15 and 27 s were utilized.

Table I - Parameters utilized to prepare the sacrificial layers. [Tabela I - Parâmetros de deposição da camada sacrificial de fotorresiste.]

Sample	Photoresist	Spin (rpm)	Time (s)	Thickness (μm)
1	AZ 1518 (diluted solution)	3000	30	1
2	AZ 1518	3000	30	2

pH sensor working electrode fabrication: intending to demonstrate the effect of the photoresist layer in the TiO₂ NT array surface, pH sensors utilizing these NT arrays as working electrode were fabricated and characterized. The measurements were performed using the TiO₂ nanotube arrays as the working electrode on a bench pH meter (HI 221, Hanna Instr.). Buffer solutions of pH 4, 5.5, 7, 8.5 and 10.0 (Hanna Instr.; buffer solutions of 5.5 and 8.5 obtained

through the mixture of 4 and 7 and 7 and 10, respectively) were used as test solutions and the sensor's electrical response (voltage between the nanotube working electrode and the Ag/AgCl reference electrode) was obtained. A linear fitting was utilized in pH response curves to obtain the pH sensor sensitivity and, to observe the hysteresis effect, a response curve measurement in a buffer solution with pH from 4 to 10 and in a sequence of 10 to 4 was done.

RESULTS AND DISCUSSION

Different TiO₂ NT growth stages: in Fig. 3 the TiO₂ NT anodization current density vs. time curve obtained for anodization voltage of 30 V for the first 100 s is shown. The three characteristic different stages are distinguished: I) in the initial anodization stage the curve presented a standard behavior where a TiO₂ compact layer grew, represented by an abrupt decrease in the current [7, 9]. Actually, the compact layer formed during the initial stage can be seen in the SEM images for anodization process times of 3.5 s (Fig. 4a) and 4.0 s (Fig. 4b). In stage II, the current density reached its minimum value and returned to increase due to the TiO₂ compact layer electrochemical dissolution by the fluorine ions [7, 9]. In this stage, it was possible to notice the nanopores (pits) formation in the TiO₂ compact layer (Figs. 4c and 4d). Finally, in stage III the current density returned to decrease slowly due to diminishing ion diffusion rate through the TiO₂ nanotubular structure [7], which in this stage was already well defined, as observed in Fig. 5.

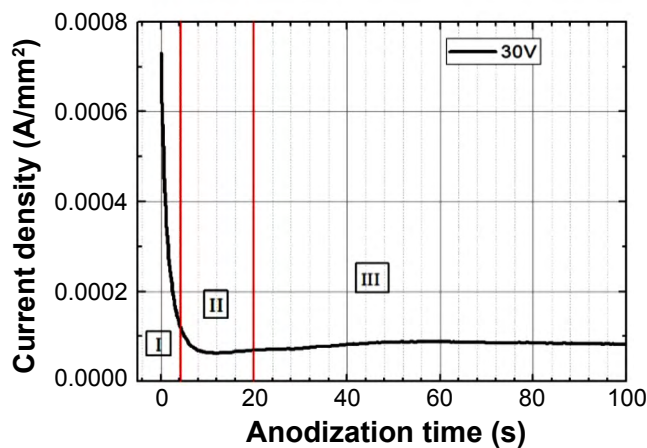


Figure 3: Anodization (J x t) curve for TiO₂ nanotubes obtained with 30 V, for the first 100 s.

[Figura 3: Curva de anodização (J x t) dos primeiros 100 s do processo de síntese dos nanotubos obtidos com 30 V.]

For higher anodization times, the TiO₂ top nanoporous layer was totally consumed and the nanotube mouth started to be attacked by the fluorine ions making the top of the nanotubes a 'nanograss' appearance. This nanograss was related with the TiO₂ compact layer that during the dissolution process became a very porous layer and remained as microflakes deposited on the nanotube mouth after the anodization process [7]. This effect occurred for any voltage

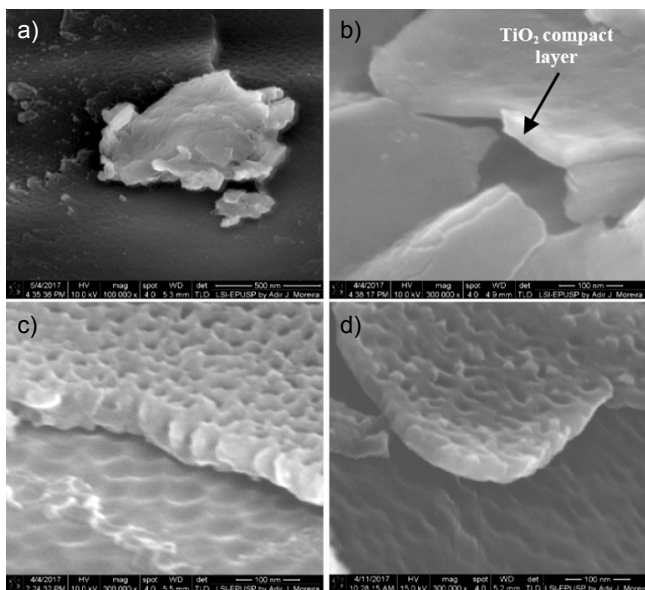


Figure 4: NTs-TiO₂ SEM images for anodization in stage I - formation of the initial compact TiO₂ layer at 3.5 s (a) and 4 s (b), and stage II - formation of nanopores (pits) at 6 s (c) and 12 s (d). [Figura 4: Imagens de MEV dos NTs de TiO₂ para o estágio I de anodização - formação da camada inicial compacta de TiO₂ em 3,5 s (a) e 4 s (b), e estágio II - formação da camada nanoporosa em 6 s (c) e 12 s (d).]

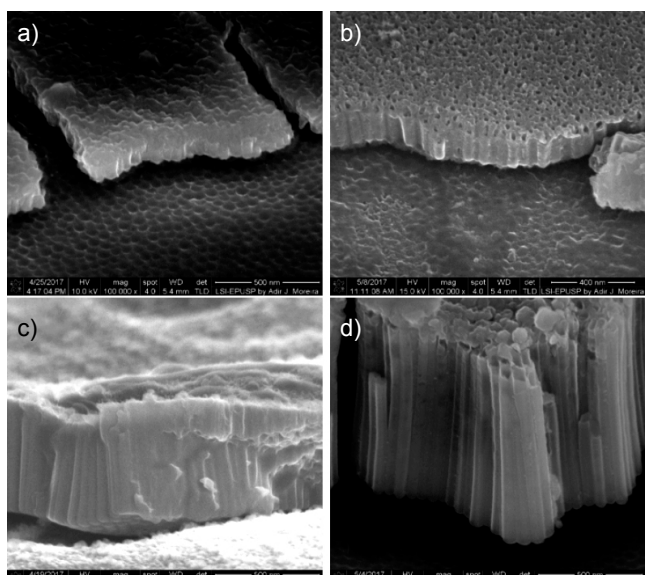


Figure 5: NTs-TiO₂ SEM images for anodization in stage III - formation of nanotubes: a) 1 min; b) 3 min; c) 6 min; and d) 15 min. [Figura 5: Imagens de MEV dos NTs de TiO₂ para o estágio III da anodização - formação dos nanotubos: a) 1 min; b) 3 min; c) 6 min; e d) 15 min.]

value, since it was correlated with the initial TiO₂ compact layer. So, for the voltage of 30 V and anodization time of 10 min, the nanopore TiO₂ layer was observed while for 30 min nanograss prevailed at the nanotube top as shown in Fig. 6.

Summarizing, the initial nanoporous layer was present while the oxidation process was dominant with respect to the chemical dissolution process. At the moment where the oxidation and the chemical dissolution reached equilibrium,

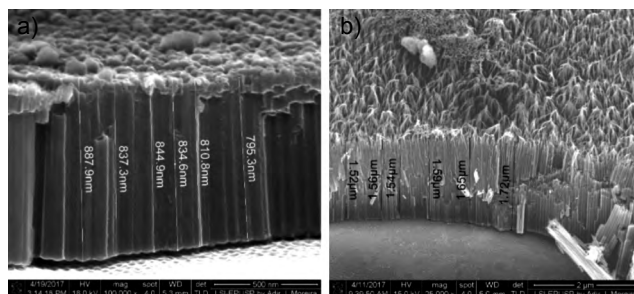


Figure 6: TiO₂ NTs obtained at 10 min (a) and 30 min (b); it is possible to observe the nanograss formation. [Figura 6: Imagens de MEV dos NTs de TiO₂ obtidos em 10 min (a) e 30 min (b); é possível observar a formação da nanograma.]

the NT surface was free and the NTs reached their maximum length value; this time was defined as process limit time. After this limit time, the chemical dissolution process was dominant and the nanotube mouth walls were attacked by the fluorine ions and as a consequence nanograss was formed in the NT mouth. In this way, to obtain nanotube mouth free of a compact nanoporous or nanograss layer, it is necessary to obtain nanotubes with a processing time close to the limit time, recalling that this parameter changes with anodization process parameters.

Method to avoid the formation of the initial compact/nanoporous TiO₂ layer: as mentioned before, to avoid the formation of the initial compact layer is necessary to reduce the initial current, which can be accomplished by the deposition of an insulating layer on the Ti foil surface. Positive photoresist (AZ1518) layers were chosen as an insulator. In order to investigate the effects of the photoresist layers on the morphology of TiO₂ NT arrays, anodization processes were carried out without and with two different photoresist thicknesses, with 60 V and 5, 15 and 30 min anodization times. Fig. 7 shows the correspondent SEM images of the TiO₂ NT top and side views. It is possible to observe the presence of the initial compact oxide layer in all samples obtained without the insulating layers process. On the other hand, completely open NT array tops were obtained for 1 and 2 μm thick layers and 15 and 30 min anodization times. The thin layer of photoresist acted as an artificial and sacrificial initial layer blocking the high initial current and sustaining most part of the applied voltage, avoiding in this way the formation of the initial compact oxide layer. As part of the applied voltage dropped on this photoresist sacrificial layer, higher process times were needed to form well defined nanotubes as observed in Fig. 7, where nanotubes wall thinning occurred slower than for NT grown without photoresist.

The mechanism for the anodization process utilizing a photoresist layer was very similar to described for TiO₂ nanotube conventional anodization. In Fig. 8 the anodization current density as a function of anodization time curves for samples obtained without photoresist layer and with 1 and 2 μm photoresist layers are shown. For samples obtained without photoresist, the Ti layer surface was directly in contact with the anodization solution and a compact

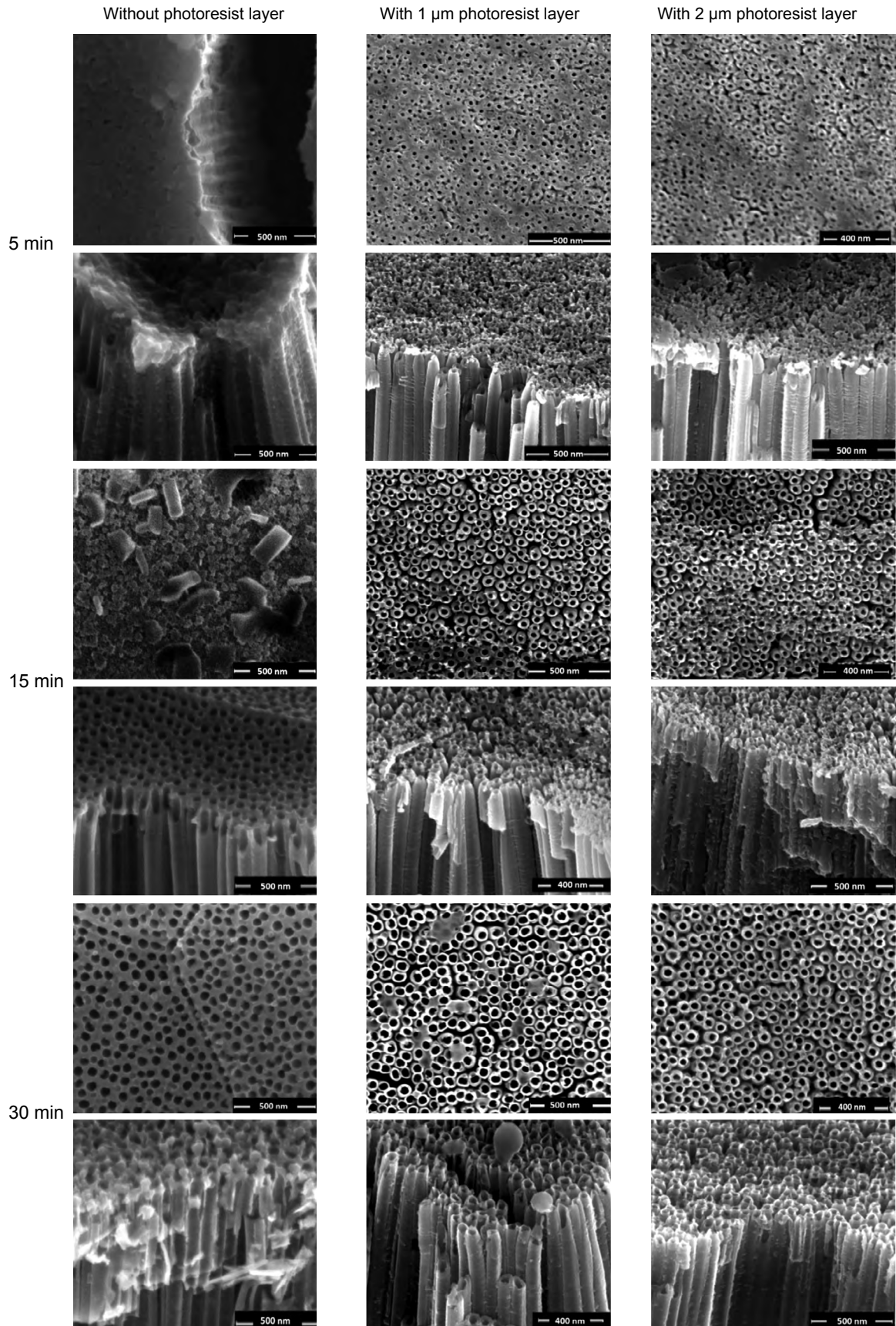


Figure 7: SEM images of TiO_2 NTs obtained for 1 and 2 μm photoresist layer thicknesses, with 60 V and anodization time of 5, 15 and 30 min. [Figura 7: Imagens de MEV dos nanotubos de TiO_2 obtidos utilizando uma camada de fotorresiste de 1 e 2 μm de espessura, com 60 V por 5, 15 e 30 min.]

oxide formed by the reaction of the Ti^+ ions, produced by the anodization voltage, with the O^{2-} originated from H_2O molecules present in the anodization solution [7, 9]. Depending on the migration rate of the Ti^{4+} and O^{2-} ionic species the growth of the new oxide occurred at the metal-oxide interface and/or at the oxide-electrolyte interface. In the case of a constant anodization voltage (V), the field $E=V.d^{-1}$ dropped constantly and decreased with the increase of the compact TiO_2 layer thickness (d), in this way an exponential decrease of the initial current with anodization time occurred. A finite thickness was reached that depended on the anodization voltage value. The Ti^{4+} injection at the oxide-electrolyte interface reacted with the fluorine ions and produced TiF_6^{2-} water-soluble species. These species were also generated by the chemical corrosion of the TiO_2 compact layer, in this way, a porous oxide and nanotube formation were observed. In this stage, an increase in anodization current was observed and increased as the reactive area increased. The ion migration rate was controlled by the oxide layer thickness; the chemical etching

process provided by fluorine ions and oxidation by oxygen ions occurred leading to nanotube formation. When a photoresist layer was utilized, the Ti surface was not exposed to the electrolyte solution avoiding, in this way, the initial compact oxide (TiO_2) layer formation on the Ti surface. In this case, the electric field E had also a constant value and thus the initial current was practically constant. An important fact was that as fluorine ions are very small, they competed with O^{2-} migration through the photoresist layer. With a higher migration rate of fluorine ions than oxygen ones, a fluorine-rich layer in the metal/photoresist interface occurred, so Ti pits formation and consequent oxidation took place, beginning the nanotube formation. In this stage, with a higher reactive area, an increase in the anodization current occurred (Fig. 8).

In order to analyze the initial anodization stages of nanotube formation with the photoresist layers, samples were obtained utilizing the photoresist layer of $1\ \mu m$ and times of 4, 15 and 27 s. In Fig. 9 SEM images of these samples are shown. Energy dispersive X-ray spectroscopy (EDS) measurements were also performed on the surface of these samples, in order to detect the presence of TiO_2 . As observed in Fig. 9a for the sample obtained at 4 s, it was not observed the presence of nanotubes and the EDS measurements for this sample also did not detect oxygen presence, indicating the absence of a titanium oxide compact layer formation. On the other hand, SEM images of samples obtained at 15 and 27 s showed that nanotubes were formed and did not present the TiO_2 compact layer; also, EDS results for the sample obtained with 15 s indicated a surface composition of 33% of Ti and 66% of oxygen. These points, 15 and 27 s, corresponded to the beginning of the current growth, the transition from stage II to stage III and, different to the case without photoresist layer, the titania formation occurred at the photoresist/Ti surface with pits of Ti surface dissolution and consequent oxidation. So, the dissolution process probably did not occur preferentially in the nanotube surface; in this case, the current growth caused the balance with the nanotube growth and the internal nanotube dissolution process. This hypothesis was reinforced as a function of nanotube mouth internal diameter and length. For nanotubes obtained with 15 s, 27 s, and 15

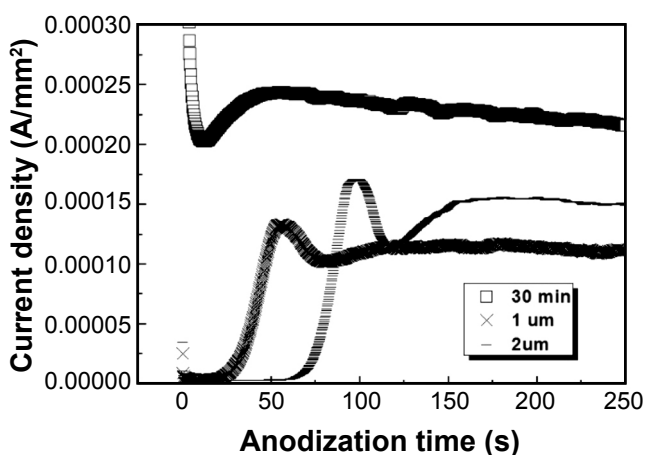


Figure 8: Current density as function of anodization time for TiO_2 NTs obtained without (30 min) and with 1 and $2\ \mu m$ photoresist layer.

[Figura 8: Densidade de corrente em função do tempo de anodização para os nanotubos de TiO_2 obtidos sem (30 min) e com a camada de 1 e $2\ \mu m$ de fotorresiste.]

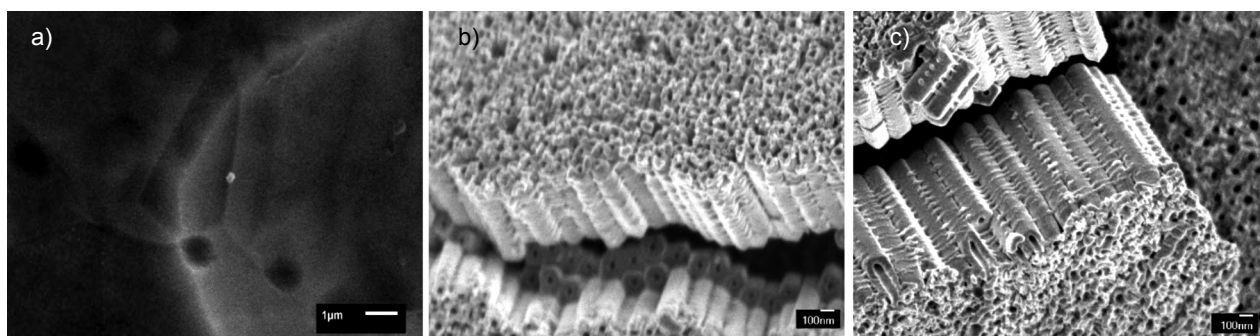


Figure 9: SEM images of samples obtained with 60 V for corresponding anodization times of 4 s (a), 15 s (b) and 27 s (c) with $1\ \mu m$ photoresist layer.

[Figura 9: Imagens de MEV das amostras obtidas com 60 V em tempos de 4 s (a), 15 s (b) e 27 s (c) utilizando camada de $1\ \mu m$ de fotorresiste.]

min, diameters of 41 ± 8 , 45 ± 7 and 37 ± 11 nm were found and the values can be considered the same under the uncertainty of diameter measurement, and the length values were 586 ± 31 , 1000 ± 28 and 2790 ± 14 nm, respectively.

In Fig. 10 the nanotube length as a function of anodization process time is shown and it is possible to observe an increase of nanotube length as a function of anodization time. This result indicated that it is possible to obtain large length nanotubes without nanograss presence, which is not possible with the conventional method as was shown in Fig. 6b. This was a consequence of the absence of compact layer formation,

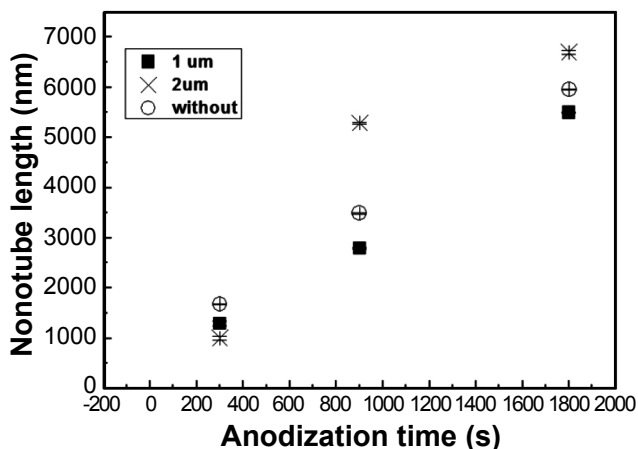


Figure 10: Nanotube length as a function of anodization time for samples obtained with 60 V and without and with 1 and 2 μm of photoresist layer.

[Figura 10: Comprimento dos nanotubos em função do tempo de anodização para as amostras obtidas com 60 V com e sem a camada de 1 e 2 μm de fotoresiste.]

which would remain as microflakes after the anodization process [7, 9, 19, 20], and due to the decrease of corrosion rate of nanotube mouths given by the protective effect of the photoresist layer. It was also observed that nanotubes obtained with 2 μm photoresist layer had longer lengths than those obtained with 1 μm of photoresist, probably due to a lower attack in nanotube surface and thus higher field-assisted oxidation in relation to the dissolution process. This can be justified observing Fig. 8 where a higher current density value was obtained for 2 μm than for 1 μm photoresist layer.

pH sensor working electrode response: pH measurements were performed in buffer solutions with pH values of 4, 5.5, 7, 8.5 and 10. In Fig. 11 the pH sensor response (for pH values of 4 to 10 and 10 to 4) for working electrodes fabricated with nanotubes obtained with 60 V for 10 and 15 min and with and without a photoresist layer is shown. As can be seen, the electrodes fabricated with the TiO_2 NTs presented a linear response with pH variation (Fig. 11). It was possible to observe that electrode fabricated with TiO_2 NT grown with a thin layer of photoresist presented better results in respect to the hysteresis effect of the electrodes fabricated with TiO_2 NTs obtained by the standard process. Analyzing the results, it was observed that electrodes obtained with a photoresist layer of 2 μm presented less hysteresis effect and a more linear behavior than those obtained with 1 μm photoresist layer. This result was attributed to the lower TiO_2 length that avoided solution trapping inside the tubes diminishing hysteresis results and improving pH sensitivity values up to approximately 52 mV/pH (Table II). It is important to observe that the worst results were obtained for a working electrode fabricated with TiO_2 NTs obtained with the standard synthesis process. As can be seen in Fig. 7, these

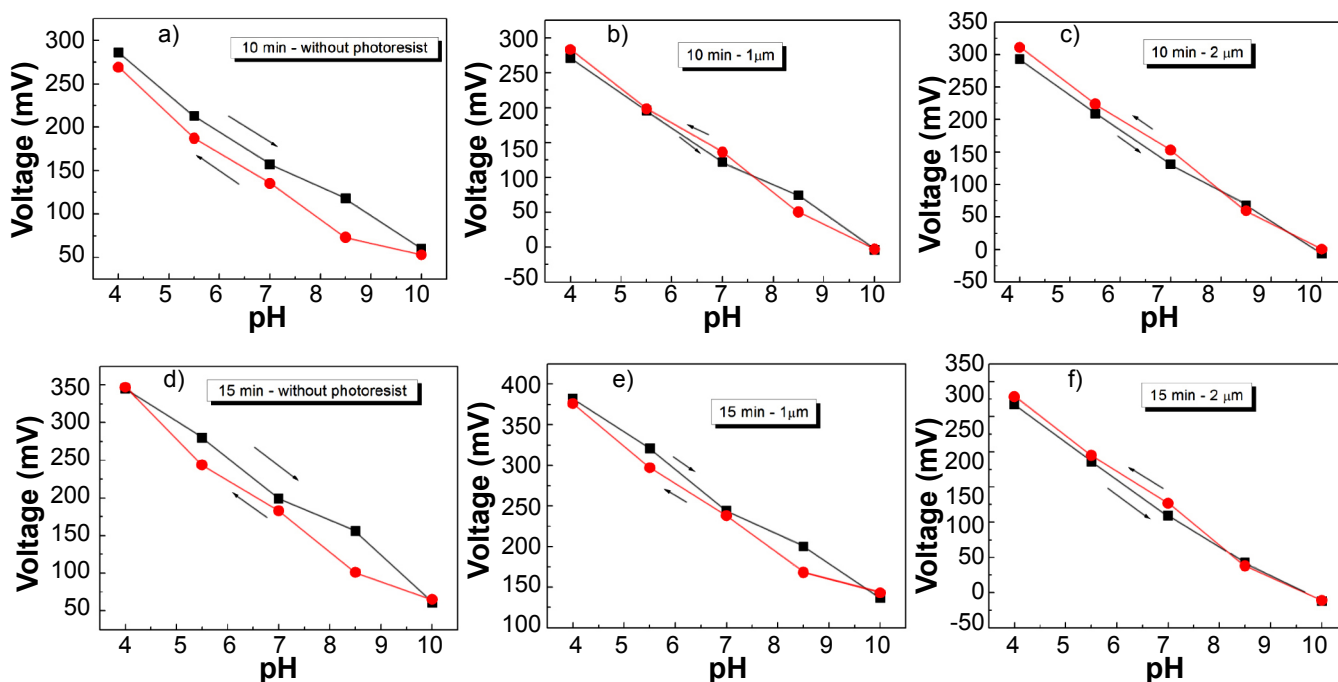


Figure 11: pH response of the TiO_2 NT electrodes.

[Figura 11: Resposta dos sensores de pH fabricados com nanotubos de TiO_2 .]

Table II - pH sensibility (mV/pH) of the TiO₂ NT electrodes.
 [Tabela II - Sensibilidade dos sensores de pH (mV/pH) fabricados com nanotubos de TiO₂.]

Anodization time	1 μm photoresist layer	2 μm photoresist layer	Without photoresist layer
10	44.8±1.8	50.0±1.4	36.4±2.1
15	40.8±1.8	46.8±2.0	47.1±4.1

NTs presented a TiO₂ initial compact layer that diffculted the penetration and trapped the solution inside the tubes, increasing hysteresis effect, and decreasing the pH sensitivity.

CONCLUSIONS

Anodic TiO₂ nanotube (NT) arrays frequently exhibit a compact, nanoporous oxide layer on the top of the arrays, attributed to the initial TiO₂ nucleation layer formed during the initial stage of the anodization process, and for long anodization process time exhibit a nanograss presence due to the dissolution of the nanotube top. This is a critical issue for many applications, because this layer affects the infiltration of materials, charge transport and recombination in the TiO₂ NTs. In this way, a modified synthesis method to avoid the formation of this layer was proposed. Prior to anodization, a thin photoresist layer was deposited on the surface of the Ti foil. Two thicknesses were investigated for anodization process carried at 60 V. This layer acted as an artificial initial layer blocking the high initial current, since most part of the applied voltage dropped on it, avoiding the nucleation of the compact TiO₂ initial layer formation. It was shown that with this technique it is possible to obtain a totally free TiO₂ NT array top surface. The optimized arrays obtained were tested as pH electrodes leading to improved sensitivity (52 mV/pH) and removal of hysteresis effects.

ACKNOWLEDGMENTS

The authors are grateful to CNPq (Process 305152/2010-6, Process 445926/2014-2 and Process 300713/90-8) and São Paulo Research Foundation - FAPESP (grant 2014/15415-4) for financial support, to Adir José Moreira of LSI/POLI-USP and CEM-UFABC for the SEM and EDS measurements.

REFERENCES

- [1] P. Xiao, Y. Zhang, B.B. Garcia, S. Sepehri, D. Liu, G. Cao, J. Nanosci. Nanotechnol. **8** (2008) 1.
 - [2] T. Froschl, U. Hormann, P. Kubiak, G. Kucerová, M. Pfanzelt, C.K. Weiss, R.J. Behn, N. Hüsing, U. Kaiser, K. Landfester, M. Wohlfahrt-Mehrens, Chem. Soc. Rev. **41** (2012) 5313.
 - [3] Q. Zheng, B. Zhou, Z. Bai, L. Li, Adv. Mater. **20** (2008) 1044.
 - [4] Z. Sun, J.H. Kim, T. Liao, Y. Zhao, F. Bijarbooneh, V. Malgras, S.X. Dou, CrysEngComm **14** (2012) 5472.
 - [5] J.Y. Kim, K. Zhu, N.R. Neale, A.J. Frank, Nano Converg. **1** (2014) 9.
 - [6] R. Zhao, M. Xu, J. Wang, G. Chen, Electrochim. Acta **55** (2010) 5647.
 - [7] P. Roy, S. Berger, P. Schmuki, Angew. Chem. Int. **50** (2011) 2904.
 - [8] J.M. Macak, H. Tsuchiya, A. Ghicov, K. Yasuda, R. Hahn, S. Bauer, P. Schmuki, Curr. Opin. Solid State Mater. Sci., **11**, 1-2 (2007) 3.
 - [9] S.P. Albu, P. Schmuki, Phys. Status Solidi **7** (2010) 151.
 - [10] J. Wang, H. Li, Y. Sun, B. Bai, Y. Zhang, Y. Fan, Int. J. Electrochem. Sci. **11** (2016) 710.
 - [11] W.H. Lee, C.W. Lai, S.B. Abd Hamid, Materials **8**, 5 (2015) 2139.
 - [12] D. Regonini, F.J. Clemens, Mater. Lett. **142** (2015) 97.
 - [13] Q.A.S. Nguyen, "Electrochemical synthesis and structural characterization of titania nanotubes", PhD Diss., Un. California, Berkeley (2010).
 - [14] R.V. Chernozem, M.A. Surmeneva, R.A. Surmevev, IOP Conf. Ser. Mater. Sci. Eng. **116** (2016) 12025.
 - [15] D. Regonini, C.R. Bowen, A. Jaroenworalluck, R. Stevens, Mater. Sci. Eng. R **74** (2013) 377.
 - [16] D. Wang, B. Yu, C. Wang, F. Zhou, W. Liu, Adv. Mater. **21** (2009) 1964.
 - [17] K. Zhu, T.B. Vinzant, N.R. Neale, A.J. Frank, Nano Lett. **7** (2007) 3739.
 - [18] K.F. Albertin, A. Tavares, I. Pereyra, Appl. Surf. Sci. **284** (2013) 772.
 - [19] R. Beranek, H. Hildebrand, P. Schmuki, Electrochem. Solid State Lett. **6** (2003) B12.
 - [20] D. Kim, A. Ghicov, P. Schmuki, Electrochem. Commun. **10** (2008) 1835
- (Rec. 22/08/2018, Rev. 29/11/2018, 01/02/2019, Ac. 02/02/2019)